

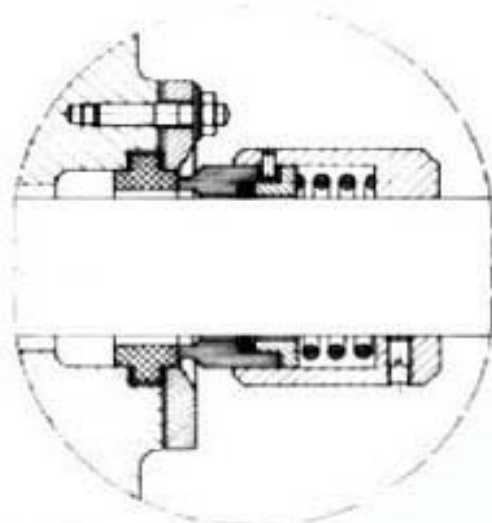


# Resistance of Oxide Ceramic Products to Corrosive Liquids

H. Mayer (Dipl.-Min.), FRIATEC AG (Mannheim)

## 1. Introduction

A typical feature of the application of oxide ceramic products in technology is its frequent key function for tools, equipment and plants. This also applies to those applications which rely on maximum operation times under corrosive conditions. **Figure 1** illustrates a classic example. Various rings made from SiC and Al<sub>2</sub>O<sub>3</sub>-ceramic are shown. Such parts are used e.g. for pumps in the chemical industry for corrosion and abrasion resistant seals and are part of the standard repertoire for special requirements made with regard to corrosion resistance. This example already points to the fact that such construction parts meet a complex range of requirements in the majority of applications and are not used with regard to one particular property alone. With a view to corrosion resistance alone, the chemical composition of the materials determines its corrosion behaviour.



Rotating mechanical seal in a chemical pump

**Figure 1:** Mechanical seal made from SiC- and Al<sub>2</sub>O<sub>3</sub>-Ceramics for chemical pumps

## 2. Corrosion Types

Corrosion processes occurring in oxide ceramic materials can be roughly subdivided into four basic types with regards to their polycrystalline microstructure:

Besides the more trivial aims of avoiding damage to the ceramic is not attacked or its complete dissolution after a short time either through an attack on the entire material or an attack only on the basic crystal in existing conditions, there is a need to emphasize the single attack on the substance at the grain boundaries of the ceramic material. That is where the material sits which does not dissolve in the basic crystal during the sintering process or which separates out from the basic crystal during cooling down from the sintering temperature. This inter-crystalline phase is naturally composed completely differently from the basic crystal itself and therefore has different chemical properties which either accelerate or slow down corrosion processes. **Figure 2** illustrates this corrosion type in model form.

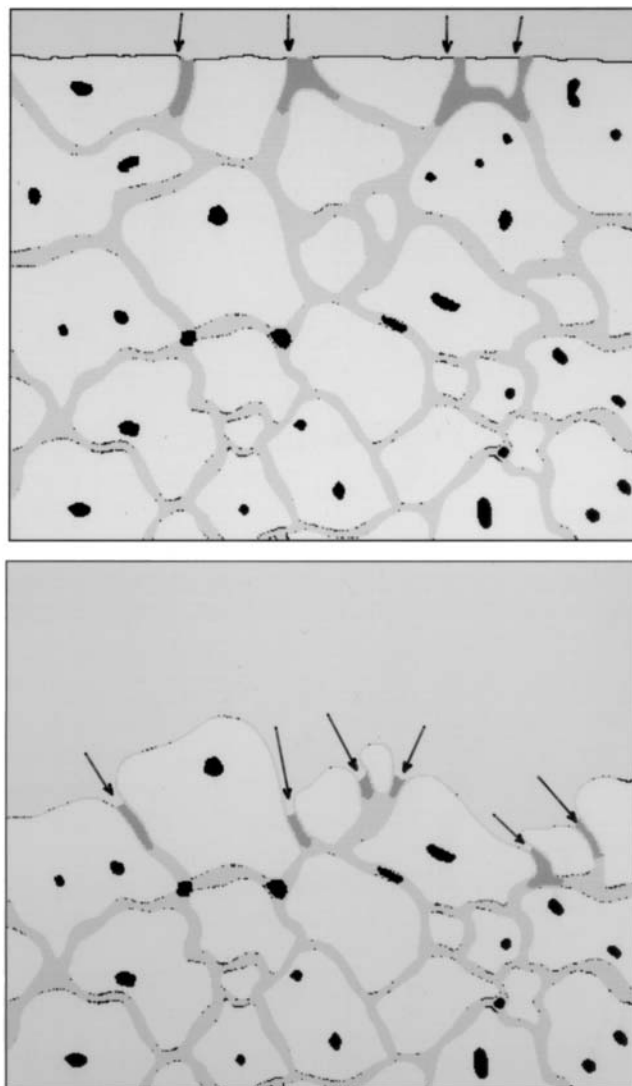


**Figure 2:** Model of intercrystalline corrosion

If the substance of the grain boundaries may be corroded in existing conditions a corrosion front will develop along the crystal boundaries which may cause the complete destruction of the material by dissolving the crystal boundary phase resulting in the crystallites falling out. While these inter-crystalline corrosion processes are not yet so advanced they are hardly noticeable macroscopically as the crystal boundaries are frequently markedly less wide than 1  $\mu\text{m}$ .

In practice e.g. lapped surfaces in that state show no changes neither in shining nor in the roughness compared to the state before the corrosion process started. In that state the strength of the material can be significantly reduced.

### 3. Determining the Corrosion Resistance

In order to test the corrosion pattern of a material, special methods need to be used. **Figure 3** gives an overview of these.

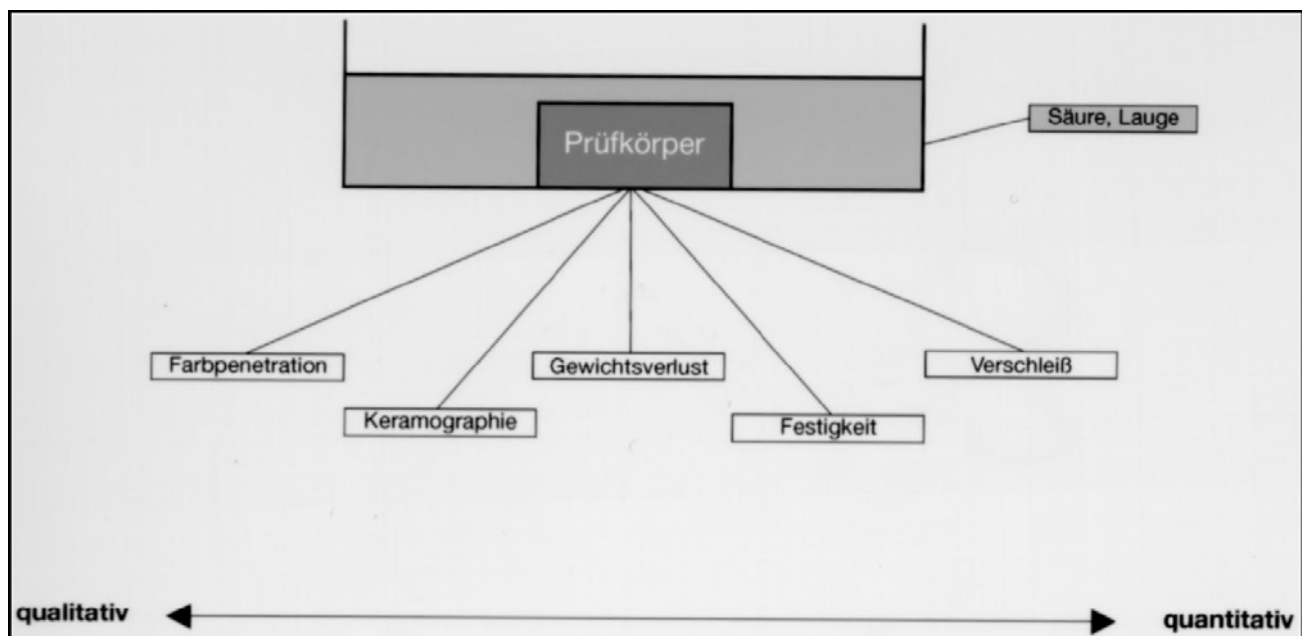


**Figure 3:** Methods for proving processes of corrosion

To test corrosion resistance of  $\text{Al}_2\text{O}_3$  ceramic FRIALIT-DEGUSSIT employs a type of test which provides a reliable result within a few days. This test involves a sample of the material to be immersed for three days in a boiling solution of 10%  $\text{H}_2\text{SO}_4$  and then dyed in an alcoholic methylene blue solution. If the grain boundaries of the material are affected by the acid a blue tinting will become visible where an extraction of the grain boundaries has also taken place.

#### 4. Effects of the Chemical Composition on Corrosion Resistance

The option of inter-crystalline corrosion leads us to believe that other materials of more than 99% purity may present a completely different corrosion pattern in certain conditions depending on origin.

In order to demonstrate this, a comparative corrosion test was carried out under above conditions on two different  $\text{Al}_2\text{O}_3$  types. The two types of material were created from the same  $\text{Al}_2\text{O}_3$  raw material with 99.8% purity and doping of 0.2%  $\text{MgO}$ , with the only difference being that one of the two types was doped additionally with 500 ppm  $\text{SiO}_2$ .

**Figure 4** shows the result of this corrosion comparison which has been recorded at different time intervals. The fact that the material type B containing more  $\text{SiO}_2$  was affected after a very short time compared to type A is clearly visible.

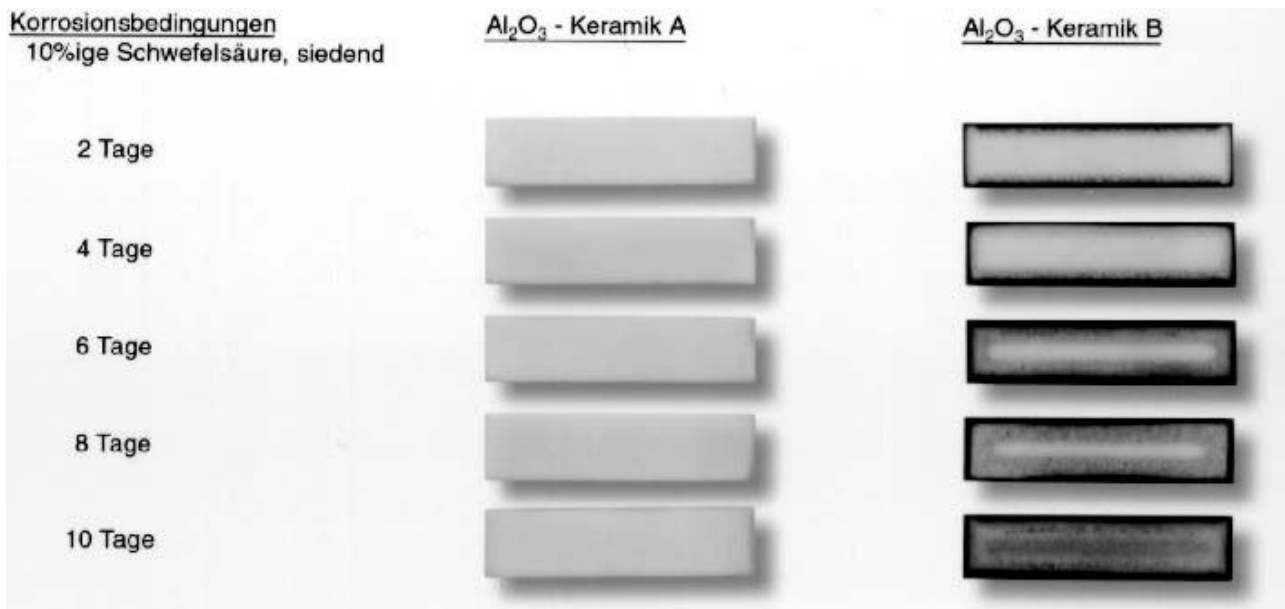


**Figure 4:** Corrosion comparison of two different  $\text{Al}_2\text{O}_3$  substances with different  $\text{SiO}_2$  concentration

A polished section was produced from sample B which had corroded for four days and been thermally etched at 1450 °C. **Figure 5** shows the surface of this sample. You can see in the corroded zone that individual crystallites are missing in the structural composition; presumably these were expelled during the sample preparation as a result of corrosion processes.

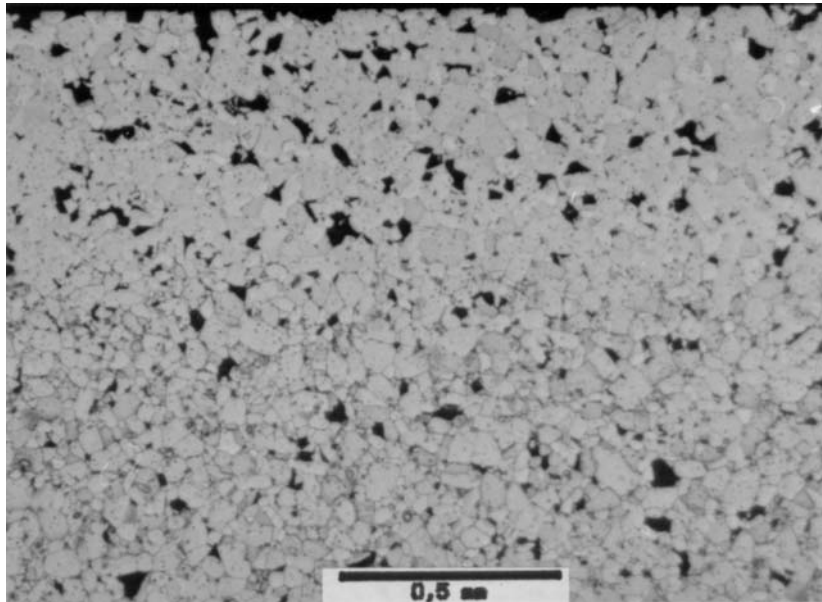


**Figure 5:** Al<sub>2</sub>O<sub>3</sub> with raised SiO<sub>2</sub> concentration after four days in seething sulfuric acid. Corroded border area, incident light.

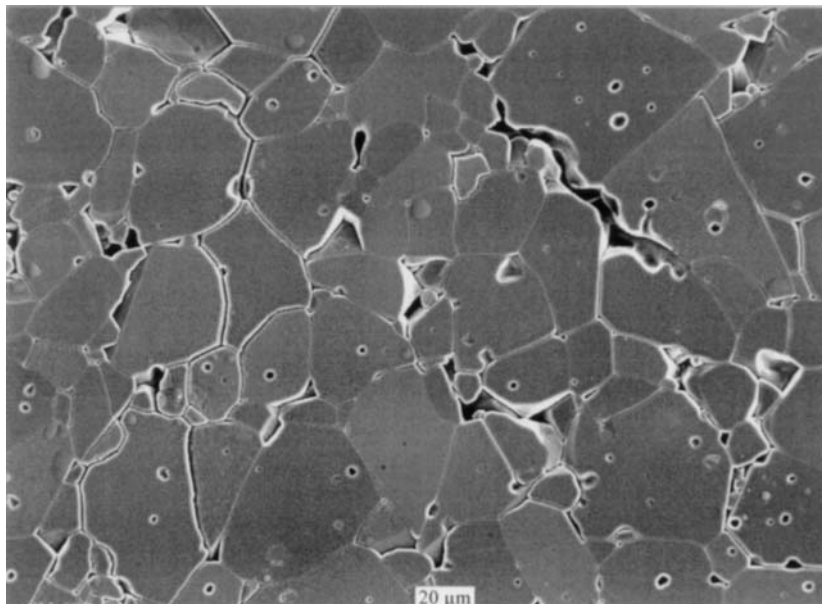


**Figure 6:** Al<sub>2</sub>O<sub>3</sub> with raised SiO<sub>2</sub> concentration after four days in seething sulfuric acid. Corrosion area, SEM.

Further enlargement in the scanning electron microscope (**Figure 6**) shows free crystal boundaries and deep gaps in places which also contain crystal boundary substance. Another noticeable feature is the hill-shaped deposits of material on the crystals (**Figure 7**). According to the results of an investigation using the electron beam microprobe the chemical composition of the grain boundary phase and the hill-shaped elevations is similar (**Figure 8, 9**).

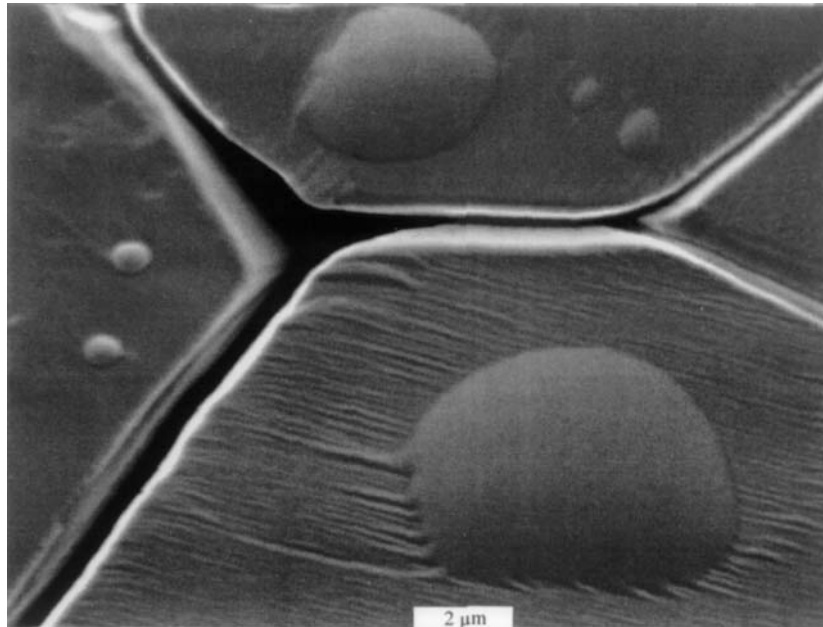


**Figure 7:** Al<sub>2</sub>O<sub>3</sub> with raised SiO<sub>2</sub> concentration after four days in seething sulfuric acid. Corrosion area. Grain boundary and aggregation of material on grain surface. SEM.

This result leads us to conclude that the deep gaps and the elevations arose only during the thermal etching process. The reason for this would appear to be a change in the viscosity of the inter-crystalline phase due to certain components dissolving during the acid treatment.

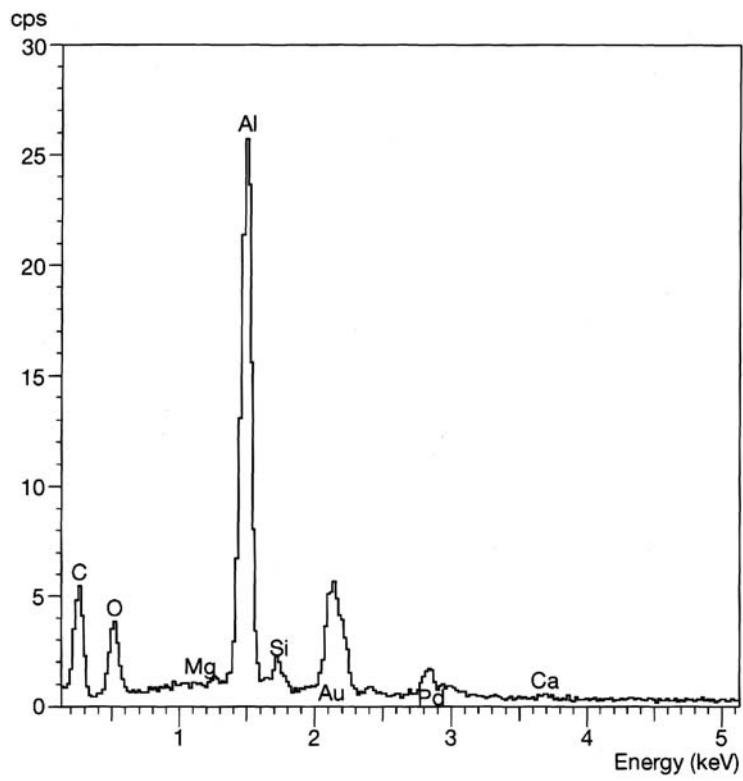


**Figure 8:** EDX-spectrum of grain boundary phase (Figure 7)

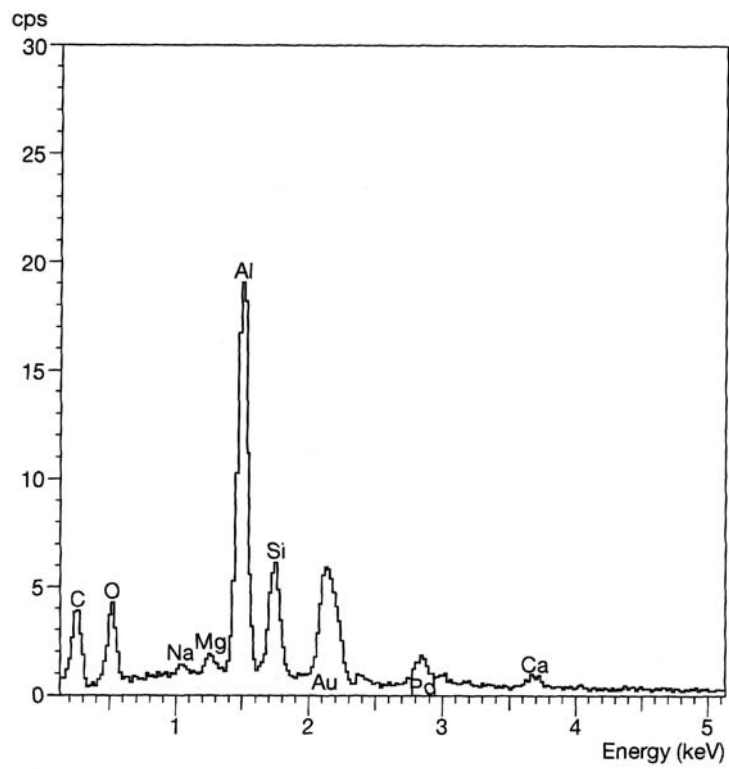


**Figure 9:** EDX-spectrum of the aggregation of material on one grain (Figure 7)

Further tests of the sample show that gaps also appear in the zone which has not been tinted (**Figure 10**), however, no material deposits can be seen on the crystal surface. This would suggest that corrosion processes have taken place in this part of the sample too which have not yet caused sufficient extraction to prevent it from being tinted.

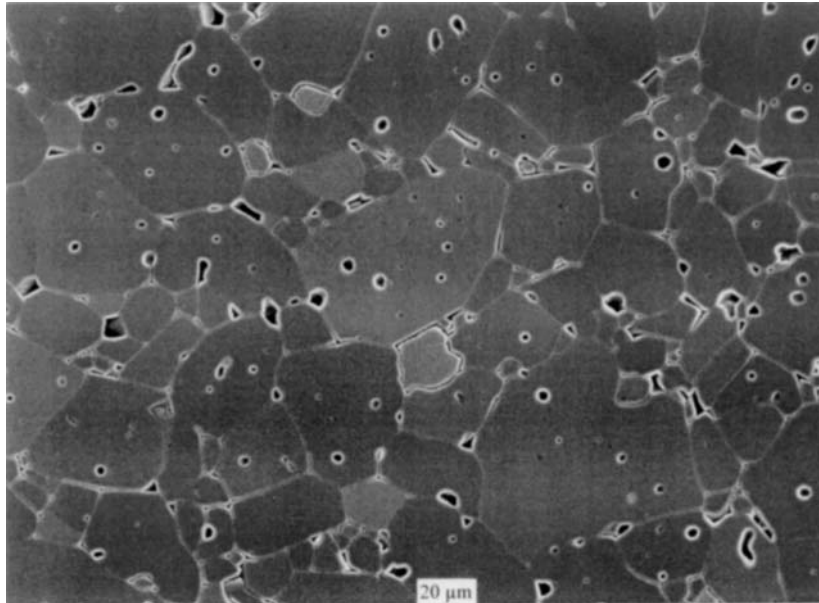


**Figure 10:** Al<sub>2</sub>O<sub>3</sub> with raised SiO<sub>2</sub> concentration after four days in seething sulfuric acid. Mid of trial.

Examining the microstructure allows differentiation of two corrosion zones, one which has not yet been extracted and an adjacent extracted zone which may be tinted due to deep damage.

If the size of the crystallites of a material can be reduced to such a degree that a grain boundary phase which may be corroded does not affect the entire ceramic structure, such a material may be made more corrosion resistant.

The simplest method to avoid such corrosion processes in principle consists of using only raw materials containing a low percentage of residual contamination as e.g. type A with a SiO<sub>2</sub> content of less than 100 ppm.

The user of oxide ceramic materials may conclude from the above that an indication of purity on its own does not guarantee corrosion resistance as the composition of the grain boundary phase is a significant aspect.

Comparative studies may help with an initial orientation when selecting corrosion resistant materials. **Table 1** shows a section from such a table as an example. Here the corrosion behaviour of Al<sub>2</sub>O<sub>3</sub> and ZrO<sub>2</sub> ceramic on the application of different media is shown in comparison with other material groups.

The real application conditions may lead to completely different results because of few changes in the composition of the chemical environment. Therefore, even today, tests under service conditions in applications play a significant role in the selection of corrosion resistant materials.

Table 1: Part of a comparative corrosion table

	Agens	chem. Formel	Konz. (%)	Temp. (°C)	Oxidkeramik			Grafit- imprägniert	PTFE	Viton	Perbunan	Neoprene	Naturkautschuk	Butyl-Kautschuk	Hyalone
					F 99,7 (Al <sub>2</sub> O <sub>3</sub> )	FZM (ZrO <sub>2</sub> )	AL 23 (Al <sub>2</sub> O <sub>3</sub> )								
01	Salzsäure	HCl	0,5	Rt	A	A	A	A	A	A	C	B	B	B	A
02			0,5	s	A	A	A	A	A	B	C	C	C	C	B
03			5	Rt	A	A	A	A	A	A	C	B	B	B	A
04			5	60	A	A	A	A	A	A	C	B	B	B	A
05			5	s	A	A	A	A	A	B	C	C	C	C	B
06			10	Rt	A	A	A	A	A	A	C	B	B	B	A
07			10	50	A	A	A	A	A	A	C	B	B	B	A
08			10	s	A	A	A	A	A	B	C	C	C	C	B
09			15	Rt	A	A	A	A	A	A	C	B	B	B	A
10			15	s	A	A	A	A	A	B	C	C	C	C	B
11			20	Rt	A	A	A	A	A	A	C	B	B	B	A
12			20	s	A	A	A	A	A	B	C	C	C	C	B
13			30	Rt	A	A	A	A	A	A	C	B	B	B	A
14			30	s	A	A	A	A	A	B	C	C	C	C	B
15			37	Rt	A	A	A	A	A	A	C	B	B	B	A
16			37	s	A	A	A	A	A	B	C	C	C	C	B
17	Salzsäure + Salpetersäure	HCl : HNO3	3:1	Rt	A	A	A	A	A	B	C	C	C	C	B
18	Schwefelchlorür	S2 Cl2		Rt	A	A	A	A	A	C	C	C	C	C	C
19				s	A	A	A		A	C	C	C	C	C	C
20	Schwefelkohlenstoff	C S2		Rt	A	A	A	A	A	A	C	C	C	C	C
21				s	A	A	A	A	A	A	C	C	C	C	C
22	Schwefelsäure	H2 SO4	2	Rt	A	A	A	A	A	A	A	A	A	A	A
23			2	s	A	A	A	A	A	A	C	A	B	A	A
24			5	Rt	A	A	A	A	A	A	A	A	A	A	A
25			5	s	A	A	A	A	A	A	C	A	B	A	A
26			10	Rt	A	A	A	A	A	A	C	C	C	B	A
27			10	s	A	A	A	A	A	A	C	C	C	C	B
28			25	Rt	A	A	A	A	A	A	C	C	C	B	A
29			25	s	A	A	A	A	A	A	C	C	C	C	B
30			50	Rt	A	A	A	A	A	A	C	C	C	B	A
31			50	s	A	A	A	A	A	A	C	C	C	C	B
32			60	Rt	A	A	A	A	A	A	C	C	C	B	A
33			60	s	A	A	A	A	A	A	C	C	C	C	B
34			77	Rt	A	A	A	A	A	A	C	C	C	B	B
35			77	s	B	C	B	C	A	A	C	C	C	C	C
36			80	Rt	A	A	A	A	A	A	C	C	C	B	B
37			80	s	B	C	B	C	A	A	C	C	C	C	C
38			85	Rt	A	A	A	A	A	A	C	C	C	B	B
39			85	s	B	C	B	C	A	A	C	C	C	C	C
40			90	Rt	A	A	A	B	A	A	C	C	C	C	B
41			90	s	B	C	B	C	A	A	C	C	C	C	C
42			96	Rt	A	A	A	B	A	A	C	C	C	B	B
43			96	s	B	C	B	C	A	A	C	C	C	C	C
44	Schwefelsäure + Salpetersäure	H2 SO4 : HNO3	10:90	35	A	A	A	C	A	B	C	C	C	C	B
45	(Mischsäure)		30:70	35	A	A	A	C	A	B	C	C	C	C	B
46			50:50	35	A	A	A	C	A	B	C	C	C	C	B
47			60:40	35	A	A	A	C	A	B	C	C	C	C	B
48			70:30	35	A	A	A	C	A	B	C	C	C	C	B
49			80:20	35	A	A	A	A	A	A	C	C	C	C	B
50			90:10	35	A	A	A	A	A	A	C	C	C	C	B
51			99:1	35	A	A	A	A	A	A	C	C	C	C	B
52	Schweflige Säure	H2 SO3	ges.	Rt	A	A	A	A	A	A	B	B	B	B	A

## 5. Examples of Applications

As mentioned at the beginning, products from oxide ceramic materials are used not only for one specific function in the majority of applications. Their strength is found in those areas where complex requirements need to be met.

Typical examples from various industrial areas for tried and tested applications are:

- a) Dosage units from 99.7%  $\text{Al}_2\text{O}_3$  ceramic for e.g. alkaline solutions, acids, medicines, pastes.
- b) Containment shells made from Mg-PSZ for magnetic coupling pumps to deliver acids and alkaline solutions in chemical plants
- c) Pressing dies made from Mg-PSZ achieve service times of more than 600 hours constant service when dry compacting highly abrasive and corrosive battery masses.
- d) The magnetically inductive flow meter shown in **Figure 11** fulfils an extremely complex range of requirements. The central component of this unit consists of a pipe from ZTA ceramic with sintered platinum cermet. Such tools allow measurement of e.g. the flow quantity of acids, alkaline solutions and abrasive deposits. Because they provide a high level of accuracy, these tools are also used in bottling plants in the drinks industry. These products today easily meet the requirements to be able to be steam sterilized and a high level of internal pressure loadability amounting to more than 1000 bar depending on manufactured size.

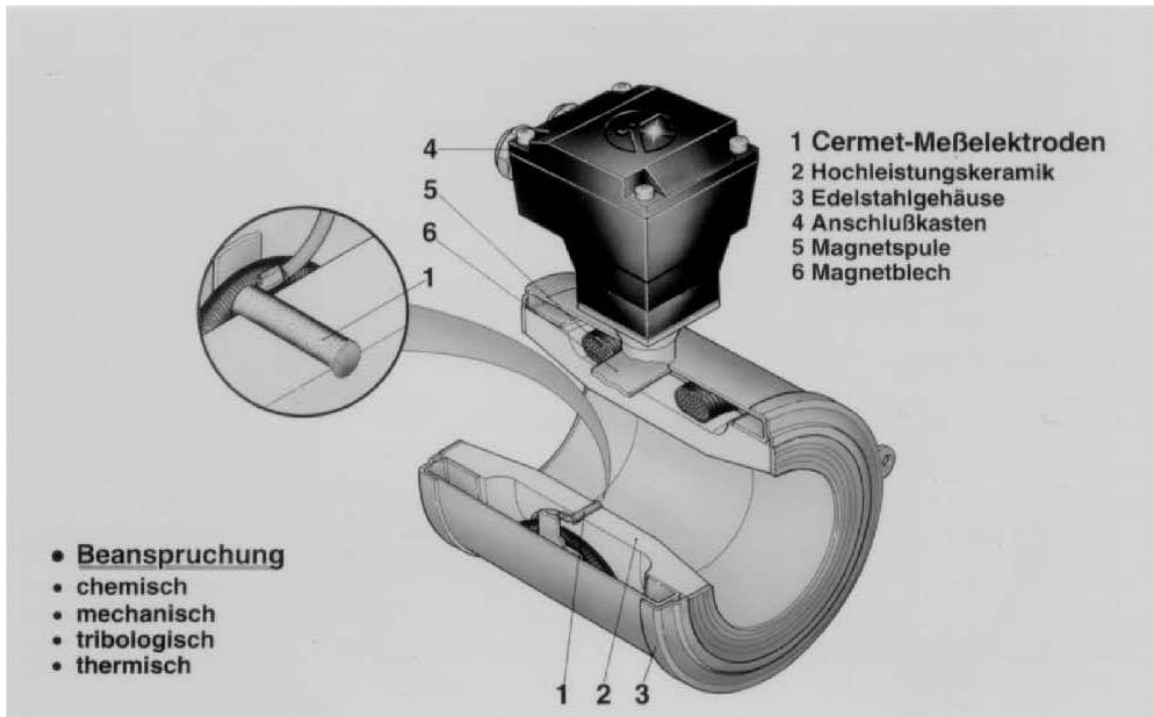


Figure 11: magnetic inductive flowmeter

## 6. Literatur

- (1) Jaeger, G., Krasemann, R.: »Beitrag zur Kenntnis des Verhaltens der Sintertonerde gegen Korrosion.« Werkstoffe und Korrosion 3 (1952), 401-415.
- (2) Dawihl, W., Klingler, E.: »Der Korrosionswiderstand von Aluminiumoxideinkristallen und von gesinterten Werkstoffen auf Aluminiumoxidgrundlage gegen anorganische Säuren.« Ber. DKG 44 (1967), 1-4.
- (3) Genthe, W., Hausner, H.: »Korrosionsverhalten von Aluminiumoxid in Säuren und Laugen.« cfi / Ber. DKG 67 (1990), 6-10.
- (4) Graas, T., Hollstein, Th., Pfeiffer, W., Reckziegel, A.: »Untersuchungen zum Korrosionsverhalten von  $\text{Al}_2\text{O}_3 + 10\% \text{ZrO}_2$  in wässrigen Lösungen.« cfi / Ber. DKG 74 (1997), 723 – 726.
- (5) FRIATEC AG, Division FRIALIT-DEGUSSIT: »Korrosionsbeständigkeit von Hochleistungs-Oxidkeramik.« Firmenprospekt Nr. 1512.5.1.90 L.